Free Radical Biology and Medicine 213 (2024) 309–321

Contents lists available at ScienceDirect

Free Radical Biology and Medicine

journal homepage: www.elsevier.com/locate/freeradbiomed

Redox modulation of oxidatively-induced DNA damage by ascorbate enhances both *in vitro* and *ex-vivo* DNA damage formation and cell death in melanoma cells

Hishyar A. Najeeb [a,1], Timi Sanusi [b], Gerald Saldanha [c], Karen Brown [a], Marcus S. Cooke [d,**], George DD. Jones [a,*]

[a] Leicester Cancer Research Centre, Department of Genetics & Genome Biology, University of Leicester, UK
[b] Leicester Medical School, University of Leicester, UK
[c] University Hospitals of Leicester NHS Trust, Leicester Royal Infirmary, UK
[d] Oxidative Stress Group, Department of Molecular Biosciences, University of South Florida, USA

ARTICLE INFO

Keywords:
Ascorbate
Oxidatively-induced DNA damage
Malignant melanoma
Comet assay
Cell death

ABSTRACT

Elevated genomic instability in cancer cells suggests a possible model-scenario for their selective killing via the therapeutic delivery of well-defined levels of further DNA damage. To examine this scenario, this study investigated the potential for redox modulation of oxidatively-induced DNA damage by ascorbate in malignant melanoma (MM) cancer cells, to selectively enhance both DNA damage and MM cell killing. DNA damage was assessed by Comet and γH2AX assays, intracellular oxidising species by dichlorofluorescein fluorescence, a key antioxidant enzymatic defence by assessment of catalase activity and cell survival was determined by clonogenic assay. Comet revealed that MM cells had higher endogenous DNA damage levels than normal keratinocytes (HaCaT cells); this correlated MM cells having higher intracellular oxidising species and lower catalase activity, and ranked with MM cell melanin pigmentation. Comet also showed MM cells more sensitive towards the DNA damaging effects of exogenous H_2O_2, and that ascorbate further enhanced this H_2O_2-induced damage in MM cells; again, with MM cell sensitivity to induced damage ranking with degree of cell pigmentation. Furthermore, cell survival data indicated that ascorbate enhanced H_2O_2-induced clonogenic cell death selectively in MM cells whilst protecting HaCaT cells. Finally, we show that ascorbate serves to enhance the oxidising effects of the MM therapeutic drug Elesclomol in both established MM cells *in vitro* and primary cell cultures *ex vivo*. Together, these results suggest that ascorbate selectively enhances DNA damage and cell-killing in MM cells. This raises the option of incorporating ascorbate into clinical oxidative therapies to treat MM.

1. Introduction

Malignant melanoma (MM)[2] is the most aggressive and deadliest of the skin neoplasms [1]. Importantly, for young people in England the incidence of melanoma has plateaued in recent decades, however it continues to rise considerably in older populations [2]. Indeed, MM incidence has quadrupled and mortality doubled since 1975, with ~16, 700 new cases and ~2,300 cancer deaths being reported per annum in the UK, making MM the 5th most common cancer in the UK [3].

Whilst >90 % of people diagnosed with MM in England survive for five years or more, the 5-year survival rate of advanced metastatic disease (stage IV) is ~30 % [4], with the advanced disease being highly refractory to current treatment modalities [5–7]. Consequently, better clinical treatments for advanced MM are needed [8,9].

Mounting evidence suggests that, compared with their normal counterparts, many types of cancer cell have increased levels of reactive

* Corresponding author. Leicester Cancer Research Centre, Department of Genetics & Genome Biology, University of Leicester, Robert Kilpatrick Clinical Sciences, Building, Leicester Royal Infirmary, PO Box 65, Leicester LE2 7LX UK
** Corresponding author. Oxidative Stress Group, Department of Molecular Biosciences, University of South Florida, Tampa, 33620, USA.
E-mail addresses: cookem@usf.edu (M.S. Cooke), gdj2@le.ac.uk (G.DD. Jones).
[1] Present address: Department of Medical Chemistry, College of Medicine, University of Duhok, Kurdistan Region-Iraq.
[2] **Non-standard abbreviations:** AA, ascorbic acid; ACA, alkaline comet assay; ALS, alkali-labile site(s); γH2AX, phosphorylated H2A.X variant histone; MM, Malignant melanoma; SB, strand break(s); ODPNL, oxidatively damaged purine nucleobase lesions(s).

https://doi.org/10.1016/j.freeradbiomed.2024.01.019
Received 19 December 2023; Received in revised form 10 January 2024; Accepted 14 January 2024
Available online 21 January 2024

oxygen species (ROS) [10–14]. Studies have shown increased levels of oxidatively damaged products, such as oxidized DNA bases and lipid peroxidation products, in clinical tumour specimens, patient plasma and cancer cell lines [15–17]. Moreover, the levels of ROS-scavenging enzymatic and non-enzymatic antioxidant defences have been shown to be significantly altered in malignant cells [18–21] and in primary cancer tissues [22,23], suggesting the aberrant regulation of redox homeostasis.

An increase in ROS in cancer is associated with abnormal cell growth and reflects a disruption of redox homeostasis due either to an increase of ROS production and/or to a decrease in ROS-scavenging capacity, leading to the condition of 'oxidative stress' (or, more accurately, "oxidative eustress") [24], with excessive oxidative stress (termed "oxidative distress") [25] leading to the detrimental damage of biomolecules and disrupted redox signalling.

Because prolonged exposure to increased ROS may contribute to the initiation and progression of cancer [11,26], oxidative stress is often viewed as an adverse event. However, excessive levels of ROS can also be toxic to cells, and cancer cells with increased oxidative stress are likely to be more vulnerable to further ROS induced by exogenous agents [27]. Therefore, increasing ROS levels in cancer cells by redox modulation, to a level that is toxic, has been proposed as a strategy to selectively kill cancer cells, overwhelming their weakened antioxidant defences and deficient repair systems, without causing significant toxicity to normal cells [28,29]. This strategy may be particularly pertinent for the treatment of MM as in melanoma cells antioxidant activity, including specifically catalase, is reported to be downregulated [30–32] and pigmented melanoma cells generate abnormally high levels of ROS, including H_2O_2, through dysregulated melanin biosynthesis [33–35]. Furthermore, the pigment melanin has an inhibitory effect on DNA repair mechanisms by reducing the functionality of DNA repair enzymes such as those involved in base excision repair (BER) pathways [36]. Additionally, melanoma cancer cells have a high affinity for redox-active metal ions due to the colloidal nature of melanin and its metal binding sites [37–39].

Ascorbate [also known as ascorbic acid (AA) and more commonly as vitamin C] is a well-known antioxidant. Its antioxidant role is largely due to its efficient scavenging of ROS and its ability to reductively replenish/recharge complementary antioxidant systems [40,41]. However, ascorbate may also lead to pro-oxidant effects, especially through the reduction of redox-active transition metal ions such as iron and copper. Upon reduction by ascorbate, these metal ions can react with H_2O_2, via Fenton reactions, to produce highly damaging hydroxyl radicals ($^{\bullet}OH$) [42,43]. $^{\bullet}OH$ reacts with DNA causing various lesions including DNA strand breaks (both single and double strand breaks; SSBs and DSBs, respectively) and oxidatively damaged nucleobase lesions [44,45]. The reactions between ascorbate and transition metals are thought to be responsible for the pro-oxidant and cytotoxic properties of ascorbate observed *in vitro* [46–48]. Ascorbate is also known to induce the release of iron bound to ferritin or haemosiderin, which could in turn promote further damaging Fenton reactions [49–52]. Additionally, AA can lead to the production of H_2O_2 via autoxidation [53,54] and hence conceivably oxidatively damaging $^{\bullet}OH$, including at pharmacologically relevant concentrations [55].

Given the potential for elevated oxidative stress in MM cells (resulting from lower antioxidant [30–32] and repair [36,56,57] activity, plus higher metal-ion content [37–39]) the aim of the present study was to examine the potential for ascorbate to increase melanoma cell killing through the enhancing of oxidant-induced DNA damage. Herein, H_2O_2 was used as a model oxidant against a panel of established MM cell lines of differing pigmentation; then extending these studies to include the pro-oxidant anti-MM agent Elesclomol (formerly STA-4783) and the *ex vivo* treatment of primary melanoma tumour cell cultures.

2. Results

2.1. Assessment of endogenous and induced DNA damage, intracellular oxidising species, catalase activity and intracellular iron levels in established MM and HaCaT cells

Elevated genome instability in cancer cells suggests a model for their selective killing via the therapeutic delivery of further damaging stress [27]. However, this strategy will likely operate best in those cancer cells already experiencing high endogenous stress and damage compared to normal cells. Accordingly, to assess the suitability of MM cells as potential target-cells for this model-scenario, the assessment of endogenous DNA damage levels in all five cell lines of the cell panel was undertaken using the alkaline Comet assay (ACA) for the detection of both strand breaks plus alkali-labile sites (SBs + ALS),[3] together with the formamidopyrimidine glycosylase (Fpg) endonuclease modified version of ACA (Fpg-ACA) for the further detection of oxidatively damaged purine nucleobase lesions (ODPNLs) measured as Fpg-sensitive sites (Fpg-ss).

There were generally higher levels of endogenous DNA damage (SB & ODPNLs) noted in all MM cells in comparison to HaCaT cells (Fig. 1A). The heavily pigmented SK23 cells had the highest endogenous damage, with all levels of damage being significantly higher compared to the corresponding levels noted for the HaCaT cells; this was followed by the moderately pigmented SK28 cells and then the two non-pigmented A375P and A375M cells, with the HaCaT cells displaying the lowest level of endogenous damage (Fig. 1A). This established an overall rank order for endogenous damage of SK23 > SK28 > A375P ≈ A375M > HaCaTs, which ranked with MM cell pigmentation levels.

The sensitivity of the MM cells to oxidant-induced damage was next assessed using ACA to assess the induction of SBs following 5–30 μM H_2O_2 treatment for 30 min on ice (Fig. 1B). The heavily pigmented SK23 cells were the most sensitive to damage, with all of the recorded levels of induced damage being significantly higher compared to the corresponding levels noted for the HaCaT cells; this was followed by the moderately pigmented SK28 cells and then the two non-pigmented A375P and A375M cells, with the HaCaT cells displaying the lowest damage sensitivity towards H_2O_2 (Fig. 1B). This established a rank order of SK23 > SK28 > A375P ≈ A375M > HaCaTs for induced damage, which again ranked with cell pigmentation and matched the rank order determined for endogenous damage.

With both the endogenous damage levels and sensitivity to induced damage in MM cells having the same rank order (see Fig. 1A and B) and correlating MM cell pigmentation, and with increased oxidative stress being proposed to be the result of increased ROS production [11–13] and/or altered antioxidant capacity [22,23,32,58], the measurement of both endogenous intracellular oxidising species by H_2DCFDA/DCF fluorescence together with an assessment of catalase activity using a qualitative visual assay [59] was undertaken in heavily pigmented SK23, non-pigmented A375P and HaCaT cell. The MM cells exhibited significantly higher levels of endogenous intracellular oxidising species than HaCaT cells, as determined by both plate reader (Fig. 1C and D) and flow cytometry (Fig. 1E) 2′,7′-dichlorofluorescein (DCF) fluorescence detection, together with significantly lower levels of catalase activity (Fig. 1F and G). This was consistent with the rank-orders for both endogenous damage and induced damage sensitivity.

With iron ions being central to the mechanism underpinning H_2O_2-induced DNA damage [54,60], it is postulated that variation in intracellular iron levels in the melanoma cancer cell lines impacts cellular sensitivity towards H_2O_2-induced DNA damage. Measurement of

[3] Hereafter, ACA detection of SB + ALS will be simply denoted as SB as, in the majority of studies, immediate SB damage makes up the majority of total strand break damage (SB + ALS) detected under alkaline conditions (see von Sonntag C. The Chemical Basis of Radiation Biology. London: Taylor & Francis; 1987).

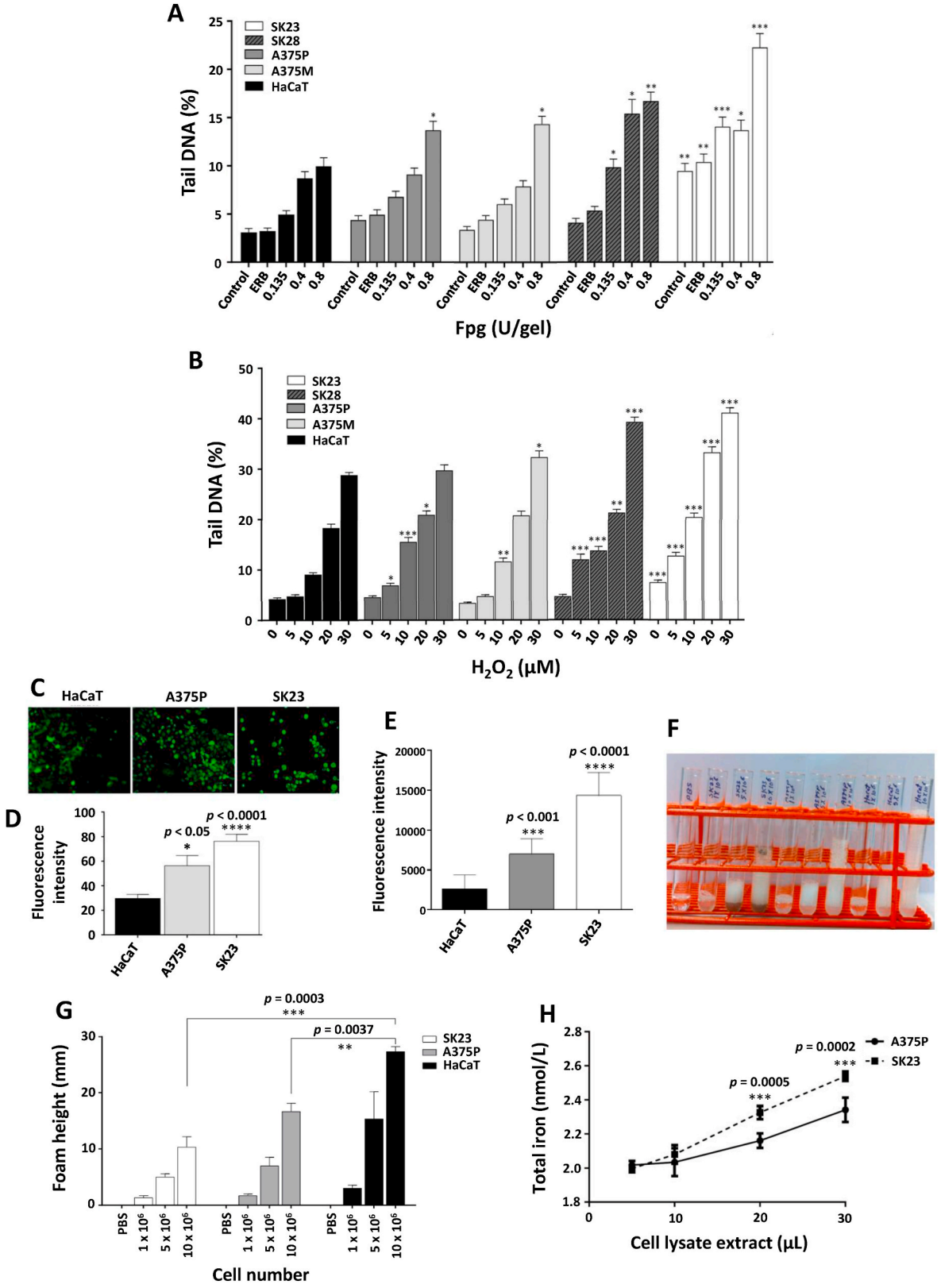

(caption on next page)

Fig. 1. Endogenous and induced DNA damage, ROS, catalase & intracellular iron levels in established MM & HaCaT cells. A). Standard ACA and Fpg-ACA assessment of endogenous DNA damage levels (SB + ODPNLs) in heavily pigmented SK28, moderately pigmented SK23, non-pigmented A375P & A375M cells and HaCaT cells (the 'cell panel'). Endogenous ODPNLs were increasingly revealed as Fpg-sensitive sites by treatment of the lysis-generated nucleoids with increasing unit amounts (per gel) of Fpg. 'Control' indicates the reporting of standard ACA; 'ERB' indicates treatment of the lysis-generated nucleoids with the Enzyme Reaction Buffer alone. One-way ANOVA compared the mean endogenous SB & SB + ODPNLs levels noted in each of the MM cells vs. the corresponding levels noted in the HaCaT cells; $*p < 0.05$; $**p < 0.005$; $***p < 0.0005$. **B).** Standard ACA assessment of H_2O_2-induced damage sensitivity, measured as induced SBs, of the cell panel following H_2O_2 treatment. Each bar indicates the mean Tail DNA (%) of 300 scored comets + SEM. One-way ANOVA compared the mean induced SB damage levels noted in each of the MM cells vs. the corresponding levels noted in the HaCaT cells; $*p < 0.05$; $**p < 0.005$; $***p < 0.0005$. **C, D & E).** Assessment of endogenous intracellular oxidising species levels. **C).** Fluorescence images indicating relative endogenous intracellular oxidising species levels in SK23, A375P and HaCaT cells. Cells were stained with H2DCFDA fluorescent probe and DCF fluorescence intensity measured by plate reader **(D)** or flow cytometry **(E)**. For both **D & E**, each bar represents mean + SD of relative fluorescence intensity determined from three independent experiments. One-way ANOVA compared the mean of fluorescence intensity for the MM cells vs. HaCaTs. **F & G).** Assessment of intracellular catalase levels in SK23, A375P and HaCaT cells. **F).** O_2-foam formation, indicative of cellular catalase enzyme activity released from the cells by lysis reacts with added H_2O_2 leading to formation of O_2-foam in the test tube. **G).** Pellets consisting of 1×10^6, 5×10^6 and 10×10^6 cells were mixed with 1 % Triton X-100 and concentrated H_2O_2 (30 %) to develop an O_2-foam and the height measured. Each bar represents mean ± SD O_2-foam height (mm). One-way ANOVA compared the mean of O_2-foam height generated by 10×10^6 MM cells vs. HaCaTs. **H)** Assessment of intracellular total iron ions in the heavily pigmented SK23 and non-pigmented A375P MM cells using the Iron Assay kit (Abacam) according to the manufacturer's instructions. Each data point represents mean ± SD of the total intracellular iron levels (nmol) per cell lysate volume (μL). T-test (unpaired) compared mean total intracellular iron levels of the two cell lines investigated.

intracellular iron levels, using an 'Iron assay kit' (Abacam), revealed that pigmented SK23 melanoma cancer cells had a significantly higher level of total intracellular iron ions than the non-pigmented A375P cells (Fig. 1H); this is consistent with the higher endogenous damage and the greater induced damage sensitivity of SK23 compared to A375P.

2.2. Ascorbate enhances H_2O_2-induced DNA damage formation & cell killing in established MM cells in vitro

With greater levels of endogenous and induced damage being noted in MM cells (Fig. 1A and B), next the potential modulating effects of ascorbate on oxidatively-induced DNA damage formation and subsequent cell killing were investigated. Cells pre-treated with or without ascorbate (100 μM) were treated with 15 μM or 30 μM of H_2O_2 on ice and SB levels assessed by ACA. For all MM cells, ascorbate caused highly significant increases in the levels of DNA damage induced by 30 μM of H_2O_2 (Fig. 2A–D); in contrast, only barely significant increases were noted for HaCaT cells (Fig. 2E). Furthermore, for the highest dose of H_2O_2 tested (30 μM) the rank order for ascorbate enhanced peroxide-induced damage was SK23 ≥ SK28 > A375P ≥ A375M > HaCaTs (Fig. 2F), paralleling both the rank orders noted for both endogenous damage (Fig. 1A) and induced damage sensitivity (Fig. 1B) and cell pigmentation. Furthermore, the extent of induced ODPNLs in SK23, SK28 and A375P cells was assessed via Fpg-ACA (Fig. 2G–I) with the levels of ascorbate-enhanced ODPNL being highest in the heavily pigmented SK23 cells (Fig. 2I: 18.5 %) and lowest in the non-pigmented A375P cells (Fig. 2G: 14.2 %); this again being consistent with the noted higher induced-damage sensitivity of SK23 compared to SK28 and

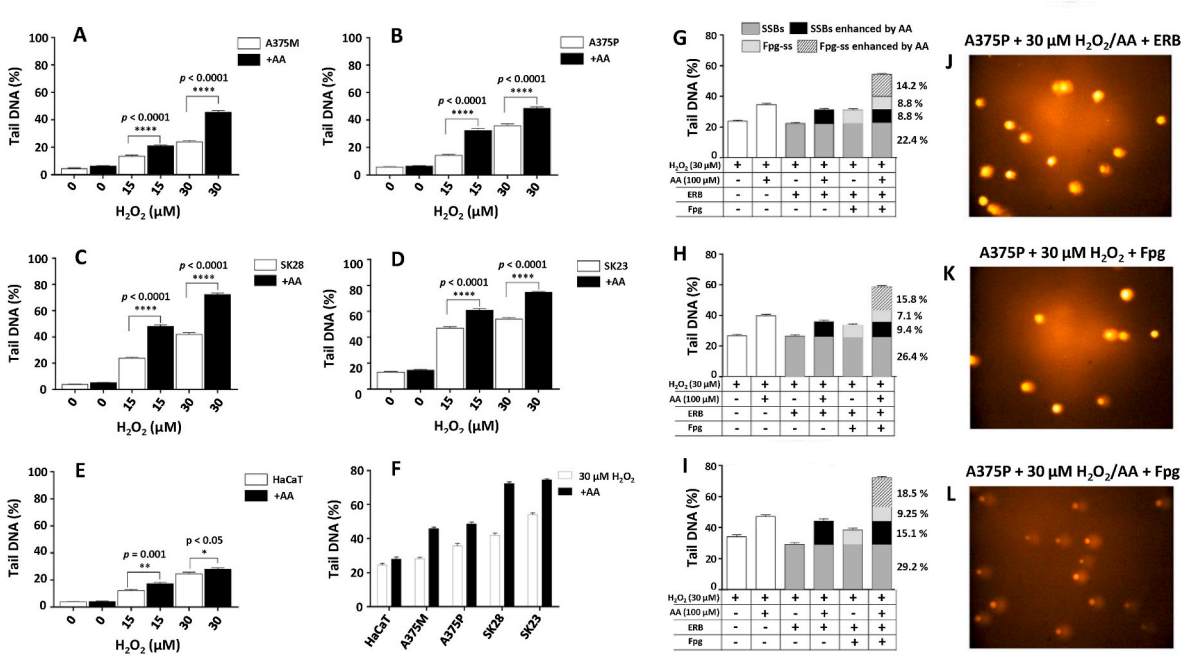

Fig. 2. Ascorbate enhances H_2O_2-induced SB and ODPNLs in established MM cells *in vitro*. A-E). MM cells (A375M **A**, A375P **B**, SK28 **C**, & SK23 **D**) & HaCaT cells (**E**) were incubated in the presence or absence of 100 μM ascorbate (2 h, 37 °C/5 % CO_2), then exposed to indicated concentrations of H_2O_2 (30 min, on ice). Cells were then assayed by ACA to assess induced SBs. Each bar indicates the mean Tail DNA (%) of 300 scored comets + SEM. One-way ANOVA compared mean levels of damage noted in the presence vs. absence of ascorbate; $*p < 0.05$, $**p < 0.01$, $***p < 0.001$, $****p < 0.0001$. **F)** Ascorbate enhancement of H_2O_2-induced SBs following pre-treatment of the cells with and without ascorbate then treatment with 30 μM H_2O_2. Each bar indicates the mean Tail DNA (%) of 300 scored comets + SEM. **G-I).** The extent of ascorbate-enhanced H_2O_2-induced ODPNLs (measured as Fpg-ss) in A375P **G**, SK28 **H** & SK23 **I**, as assessed by Fpg-ACA. Each bar indicates the mean Tail DNA (%) of 300 comets + SEM. **J-L).** Representative fluorescent images of comets following treatment of A375P cells with ascorbate and then 30 μM H_2O_2 with the lysis-generated nucleoids being treated with ERB **J**, with H_2O_2 alone and subsequently the lysis-generated nucleoids being treated with Fpg **H**, with ascorbate and then H_2O_2 and the lysis-generated nucleoids being treated with Fpg **L**.

A375P (Fig. 1B) and again ranking MM cell pigmentation.

On the basis that ascorbate enhances both H_2O_2-induced SB and ODPNLs formation in MM cells (Fig. 2A–D & 2G-I), it was proposed that ascorbate may also enhance H_2O_2-induced DSBs in MM cells. The cell panel was again pre-treated with or without ascorbate (100 μM) and then treated with 15 μM or 30 μM of H_2O_2 on ice and DSB levels were assessed by γ-H2AX foci formation. For all MM cells, ascorbate significantly enhanced the levels of DSBs induced by 30 μM of H_2O_2 (Fig. 3C–F); in contrast, no significant increase was noted for HaCaT cells (Fig. 3G). Furthermore, for the highest dose of H_2O_2 tested (30 μM), the rank-order for ascorbate enhanced H_2O_2-induced DSBs was SK23 > SK28 > A375P > A375M > HaCaTs (Fig. 3H), matching the rank-order for ascorbate enhancement of peroxide-induced SBs (Fig. 2F) and again ranking with cell pigmentation.

Given that ascorbate enhances H_2O_2-induced DSBs (Fig. 3H) and that DSBs are one of the most lethal lesions induced by genotoxic agents [61], it was further proposed that ascorbate may also enhance H_2O_2-induced MM cell killing. Therefore, a clonogenic assay was used to measure MM and HaCaT cell survival following treatment with H_2O_2 (10–40 μM) after pre-treatment with or without ascorbate (100 μM). Examination of the clonogenic data showed that ascorbate enhanced H_2O_2-induced cell killing of all MM cells (Fig. 3I-L), with the greatest enhancement of cell killing being noted for SK23 cells (Fig. 3L) and the lowest for A375M cells (Fig. 3I), whilst concomitantly exerting a protective effect towards HaCaT cells (Fig. 3M). This again parallels the rank-order for ascorbate enhancement of peroxide-induced DSBs in MM cells (Fig. 3H) and again ranks with MM cell pigmentation.

2.3. Ascorbate enhances Elesclomol-induced DNA damage formation in established MM cells in vitro and in primary MM cell cultures ex vivo

Elesclomol is an investigational drug that exerts potent anticancer activity through the elevation of ROS levels [62] and has undergone clinical evaluation as a possible anticancer therapeutic [63–66]. Elesclomol generates oxidative stress by binding to cupric copper ions (Cu^{2+}) forming an extracellular Elesclomol-Cu^{2+} complex than enables transport into the cell and localisation in the mitochondria [67]. Upon entering the mitochondria, the copper is reduced to cuprous Cu^{1+} and is released, facilitating the initiation of redox reactions that may propagate oxidative stress [68]. This was confirmed in the current study when the antioxidant NAC was noted to abolish the oxidising effects of Elesclomol (500 nM) in heavily pigmented SK23 cells (Fig. 4A). Importantly, Elesclomol has demonstrated oxidative stress-mediated cell killing in melanoma cancer cells [69] and so it was proposed that ascorbate may enhance Elesclomol-induced DNA damage formation in MM cells.

SK23, SK28 and A375P cells were treated with 50 or 100 nM Elesclomol following pre-treatment with or without ascorbate (100 μM) and ACA used to measure Elesclomol-induced DNA damage. Ascorbate treated MM cells showed an enhancement of Elesclomol-induced DNA damage (Fig. 4B–D) with both the Elesclomol-induced and ascorbate-enhanced DNA damage being highest in heavily pigmented SK23 melanoma cancer cells (Fig. 4D) and lowest in the non-pigmented A375P cells (Fig. 4B); paralleling the rank-order for ascorbate enhancement of H_2O_2-induced SB damage (Fig. 2F). Furthermore, Fpg-ACA analysis of the SK23 response towards Elesclomol following ascorbate pre-treatment indicated the enhanced formation of ODPNLs (Fig. 4E: 10.6 %), revealing that the enhancement of Elesclomol-induced DNA damage by ascorbate is mediated by superimposing oxidatively damaging events.

With the above studies demonstrating that ascorbate enhances Elesclomol-induced oxidatively damaged DNA in established MM cells *in vitro*, the present study was extended to an examination of primary MM cell cultures *ex vivo*. Six metastatic melanoma tissue samples were obtained via surgical excision of cutaneous melanoma tissue. Histopathological examination was conducted to determine viable tumour tissue and lesion characteristics (Table 1). Disaggregation was performed upon delivery of the samples to the lab, generating cell suspensions suitable for treatment. Cells from three tissue samples [two pigmented (denoted B33 & B46) and one non-pigmented (denoted B45)] were treated with 50 μM of H_2O_2 following pre-treatment with or without ascorbate (100 μM) and SB levels assessed by ACA; similarly, cells from the remaining three tissue samples [again, two pigmented (denoted B57 & B64) and one non-pigmented (denoted B63)] were treated with Elesclomol following pre-treatment with or without ascorbate (100 μM) and SB levels again assessed by ACA. Generally, higher doses of Elesclomol were required for the treatment of the primary cell cultures, typically 50 μM (and exceptionally 1 mM to observe induced damage over and above the high background noted in B57). Nevertheless, for all the pigmented primary sample-cells, ascorbate significantly enhanced the levels of DNA damage induced by both H_2O_2 (Fig. 5B and C) and Elesclomol (Fig. 5E and F); in contrast, either a smaller and less or no significant increases were noted with the non-pigmented primary sample cells (Fig. 5D and G).

3. Discussion

The effectiveness of current anti-MM gene-targeted therapeutic strategies is limited by drug resistance and the genomic instability that MM cancer cells acquire [70,71]. Therefore, novel approaches to anti-MM cancer therapeutics must be innovative and take advantage of new fundamental discoveries. Research concerning ascorbate and its anticancer functions continues to gain traction, be it through induction of redox imbalance, metabolic stress and energy crisis [72–74], epigenetic modulation [75–77] or sensitisation of cancer cells [78,79]. Therefore, the current study actively contributes to the growing body of research with respect to ascorbate and its therapeutic potential.

3.1. Elevated levels of endogenous and induced oxidative stress in pigmented MM cells

This study demonstrated that MM cells possess elevated levels of endogenous oxidatively damaged DNA compared to other non-cancer skin cells i.e., HaCaT keratinocytes, with the heavily pigmented SK23 cells having the highest level of endogenous damage and the noted rank order being SK23 > SK28 > A375P ≈ A375M > HaCaTs (Fig. 1A) which parallels cell pigmentation. Furthermore, an identical rank order was noted for exogenous H_2O_2-induced damage formation (Fig. 1B), with this again paralleling MM cell pigmentation.

Given the same rank order for both endogenous and induced DNA damage and this associating with cell pigmentation, it was proposed that pigmented MM cells could have higher levels of endogenous ROS and/or decreased antioxidant defence compared to non-pigmented MM cells and/or HaCaT keratinocytes. This was clearly demonstrated by the SK23 cells having both significantly higher levels of endogenous intracellular oxidising species (Fig. 1D and E) and lower levels of intracellular catalase enzyme activity (Fig. 1G) compared to non-pigmented A375P and HaCaT cells; the latter observation supporting the observation of weakened antioxidant defences in tumour cells [80,81]. Our experiments further show that intracellular iron ions may play a role in H_2O_2-induced DNA damage in MM cells [60] with the heavily pigmented SK23 cells having a significantly higher iron content than the non-pigmented A375P MM cells (Fig. 1H).

In support of the above, it has been reported that in MM cells enzyme antioxidant activity, such as that of catalase, is downregulated [30–32] and that pigmented MM cells generate abnormally high levels of ROS, including H_2O_2, through dysregulated melanin biosynthesis [33–35]. Furthermore, MM cells have a high affinity for redox-active metal ions due to the colloidal nature of melanin and its metal binding sites [37–39].

Taken together our data suggests that pigmentation, through elevated iron and intracellular oxidising species levels, together with reduced catalase enzyme antioxidant defence, may be associated with

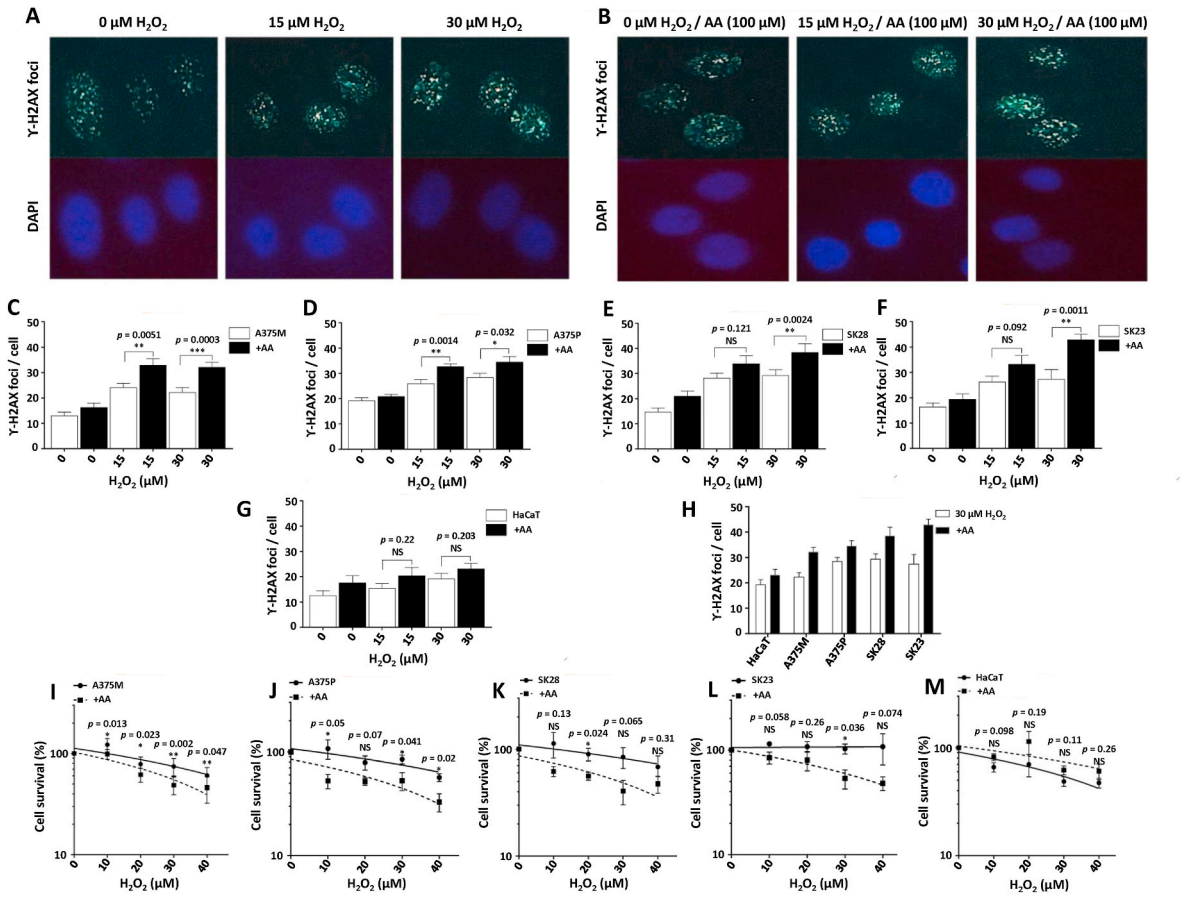

Fig. 3. Ascorbate enhances H_2O_2-induced DSBs and cell killing in established MM cells *in vitro*. A & B). Representative fluorescent images of γ-H2AX foci (green) and DAPI stain (blue) nuclei of A375M cells pre-treated with or without ascorbate (100 μM, 2 h, 37 °C/5 % CO_2) then exposed to 15 μM and 30 μM H_2O_2 (30min on ice). **C-G).** MM and HaCat cells (A375M **C**, A375P **D**, SK28 **E**, SK23 **F** & HaCaT **G**), seeded on coverslips, were incubated in the presence or absence ascorbate then exposed to H_2O_2 as indicated above. The cells were then methanol fixed (24 h at −20 °C) before γ-H2AX immunoassay/foci counting (see Materials & Methods). Each bar represents mean + SEM of γ-H2AX foci number per cell determined from 10 fields. *T*-test (unpaired) compared mean γ-H2AX foci number noted in the presence vs. absence of ascorbate. NS, non-significant, $*p < 0.05$, $**p < 0.01$, $***p < 0.001$ *versus* ascorbate untreated cells. **H).** Ascorbate enhancement of H_2O_2-induced DSBs following cell treatment with 30 μM H_2O_2. **I-M).** Clonogenic survival (%) of A375M **I**, A375P **J**, SK28 **K**, SK23 **L** and HaCaT **M;** cells were treated with (or without) ascorbate (100 μM, 2 h, 37 °C/5 % CO_2) then exposed to the indicated concentrations of H_2O_2 (30 min, on ice). Cells were then seeded and incubated at 37 °C/5 % CO_2 to develop colonies. Old media was replaced with fresh every 6 days until visible colonies appeared, which were then stained and counted. Each point represents mean ± SD of survival (%). *T*-test (unpaired) compared the mean of survival between the ascorbate treated *versus* untreated cells.

greater susceptibility to oxidant-induced DNA damage in MM cells, and that further exposure to and/or the modulated-enhancement of 'therapeutic ROS' may exacerbate the inherently high levels of oxidatively damaged DNA in MM cells and so selectively exceed damage-threshold for cell survival and so achieve selective MM cell killing.

3.2. *Ascorbate enhances H_2O_2-induced DNA damage formation to achieve the selective cell killing of MM cells*

For all MM cells, pre-treatment with ascorbate caused highly significant increases in the levels of DNA SB damage induced by H_2O_2 (Fig. 2A–D). This is in agreement with previous work demonstrating the pro-oxidant functions of ascorbate [47,54,82,83]. Also, the rank order for ascorbate-enhanced H_2O_2-induced DNA damage (Fig. 2F; SK23 ≥ SK28 > A375P ≥ A375M > HaCaTs) was noted to match that for endogenous damage and induced damage sensitivity. Furthermore, Fpg-ACA analysis revealed the levels of ascorbate-enhanced ODPNLs to be highest in the heavily pigmented SK23 cells, lower in SK28 cells and lowest in the non-pigmented A375P cells (Fig. 2G–I), confirming the enhancement of H_2O_2-induced oxidatively damaged DNA in MM cells by ascorbate.

Subsequent γ-H2AX immunoassay analysis demonstrated that, for all MM cells, ascorbate significantly enhanced the levels of DSBs induced by 30 μM H_2O_2 (Fig. 3C–F) with again the same rank order for ascorbate-enhanced DSB damage (Fig. 3H; SK23 > SK28 > A375P > A375M > HaCaTs) being noted as for ascorbate-enhanced SB damage (Fig. 2F).

With DSBs being one of the most lethal lesions induced by genotoxic agents [61], our data proposes that pre-treatment of MM cells with pharmacologically relevant levels of ascorbate will enhance H_2O_2-induced cell killing. Indeed, clonogenic analysis revealed that ascorbate enhances H_2O_2-induced cell killing of all MM cells (Fig. 3I-L), with the highest enhancement being noted for SK23 cells (Fig. 3L) and the lowest for A375M cells (Fig. 3I), matching ascorbate's enhancement of peroxide-induced DSBs in MM (Fig. 3H), whilst concomitantly exerting a protective effect towards HaCaT cells (Fig. 3M).

Taken together this data further substantiates the above findings that pigmented MM cells are more sensitive to H_2O_2-induced DNA damage and its enhancement by ascorbate, with this in turn rendering them more susceptible to cell death under the oxidative conditions potentiated by ascorbate. These observations are supported by studies indicating that induced oxidatively damaged DNA initiates apoptotic mechanisms mediated by H_2O_2 [84,85]. More specifically, H_2O_2/model oxidant-induced oxidative stress potentiates the expression of effector caspase proteins (Caspase 3 and 7) [86,87] which are well established

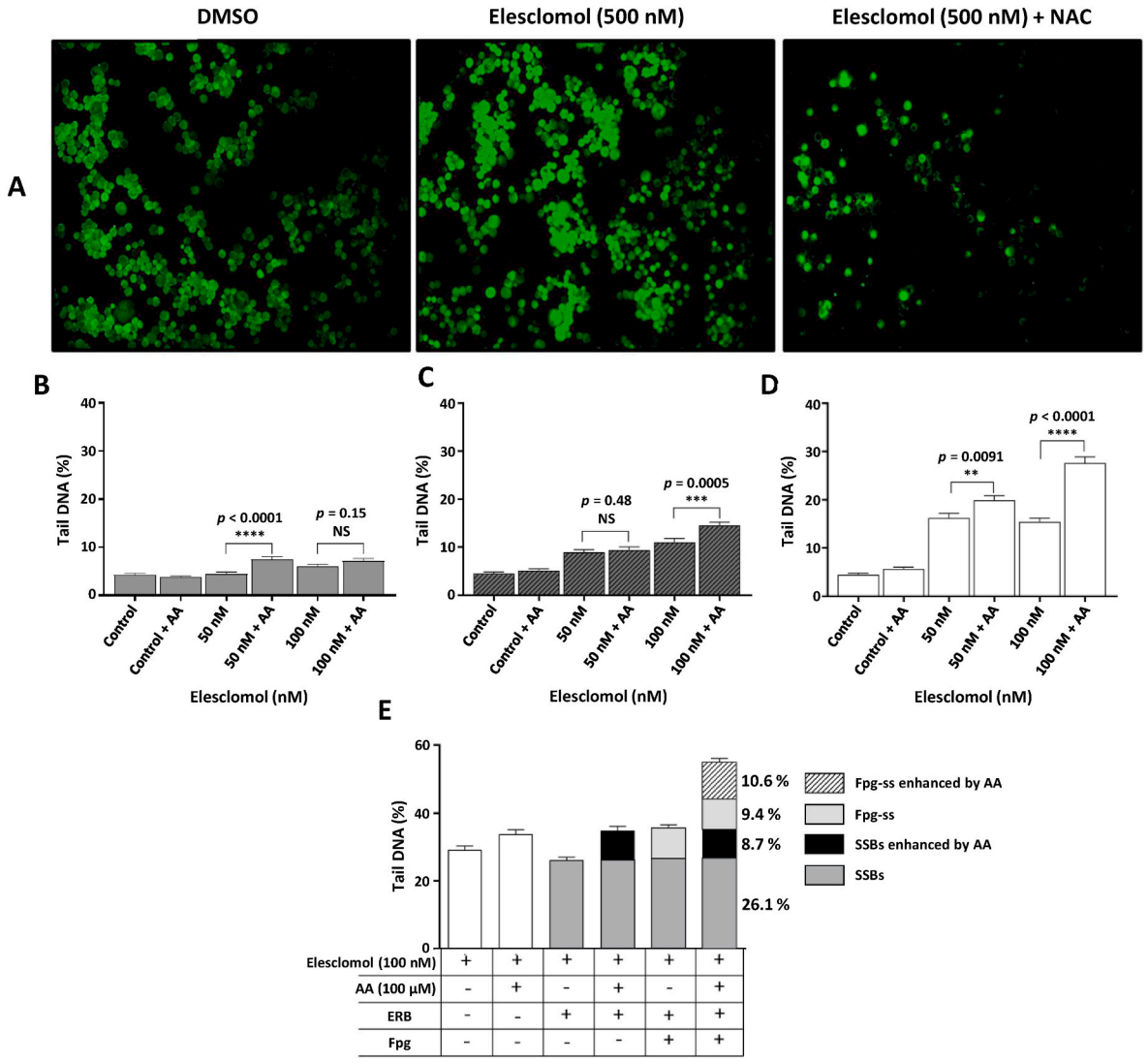

Fig. 4. Ascorbate enhances Elesclomol-induced oxidatively damaged DNA in established MM cells *in vitro*. A). Assessment of Elesclomol-induced ROS levels; representative DCF fluorescence images indicating relative intracellular oxidising species levels in SK23 cells following Elesclomol treatment (7 h at 37 °C/5 % CO_2) with one group of Elesclomol-treated cells exposed to the antioxidant NAC (500 µM, 30 min, 37 °C/5 % CO_2) before H_2DCFDA addition. **B-D).** Ascorbate enhances Elesclomol-induced DNA damage in A375P **B**, SK28 **C** and SK23 **D**. The cells were incubated with and without ascorbate and then exposed to the indicated concentrations of Elesclomol and DNA damage measured by ACA. Each bar represents the mean Tail DNA (%) of 300 comets + SEM. T-test compared the difference between the means of induced DNA damage for ascorbate treated cells vs. ascorbate untreated cells; NS, non-significant, $*p < 0.05$, $**p < 0.01$, $***p < 0.001$, $****p < 0.0001$. **E).** The extent of ascorbate-enhanced Elesclomol-induced ODPNLs (measured as Fpg-ss) in SK23 cells as assessed via Fpg-ACA following ascorbate and Elesclomol treatment (see above). Each bar shows the mean Tail DNA (%) of 300 comets + SEM.

Table 1
Melanoma tissue sample characteristics.

Participant ID	Gender	Age	Sample location	Lesion description
B33	**Female**	**76**	**Regional (axilla) lymph node metastasis**	**Pigmented**
B45	**Female**	**53**	**Regional (axilla) lymph node metastasis**	**Non-pigmented**
B46	**Female**	**41**	**Regional skin metastasis**	**Pigmented**
B57	**Male**	**75**	**Regional (groin) lymph node metastasis**	**Pigmented**
B63	**Male**	**75**	**Regional (axilla) lymph node metastasis**	**Non-pigmented**
B64	**Male**	**73**	**Regional (axilla) Lymph node metastasis**	**Pigmented**

markers for apoptosis [88–90]. Significantly, there is evidence to suggest that these oxidant-induced apoptotic mechanisms may operate in MM cells [91].

3.3. Ascorbate selectively enhances Elesclomol-induced oxidatively damaged DNA in pigmented MM cells in vitro and in pigmented primary MM cell cultures ex vivo

The drug Elesclomol has been reported to induce oxidative stress in cancer cells, including MM cells, through the augmentation of endogenous intracellular ROS [62]. This was confirmed in the current study when the antioxidant NAC was noted to abolish the oxidising effects of Elesclomol in heavily pigmented SK23 cells (Fig. 4A). The utility of Elesclomol has been studied in clinical trials to treat advanced MM cases [65,66,92,93], but there was no indication of significant improvement in progression free survival in these patients. However, these trials examined Elesclomol in combination with Paclitaxel, a

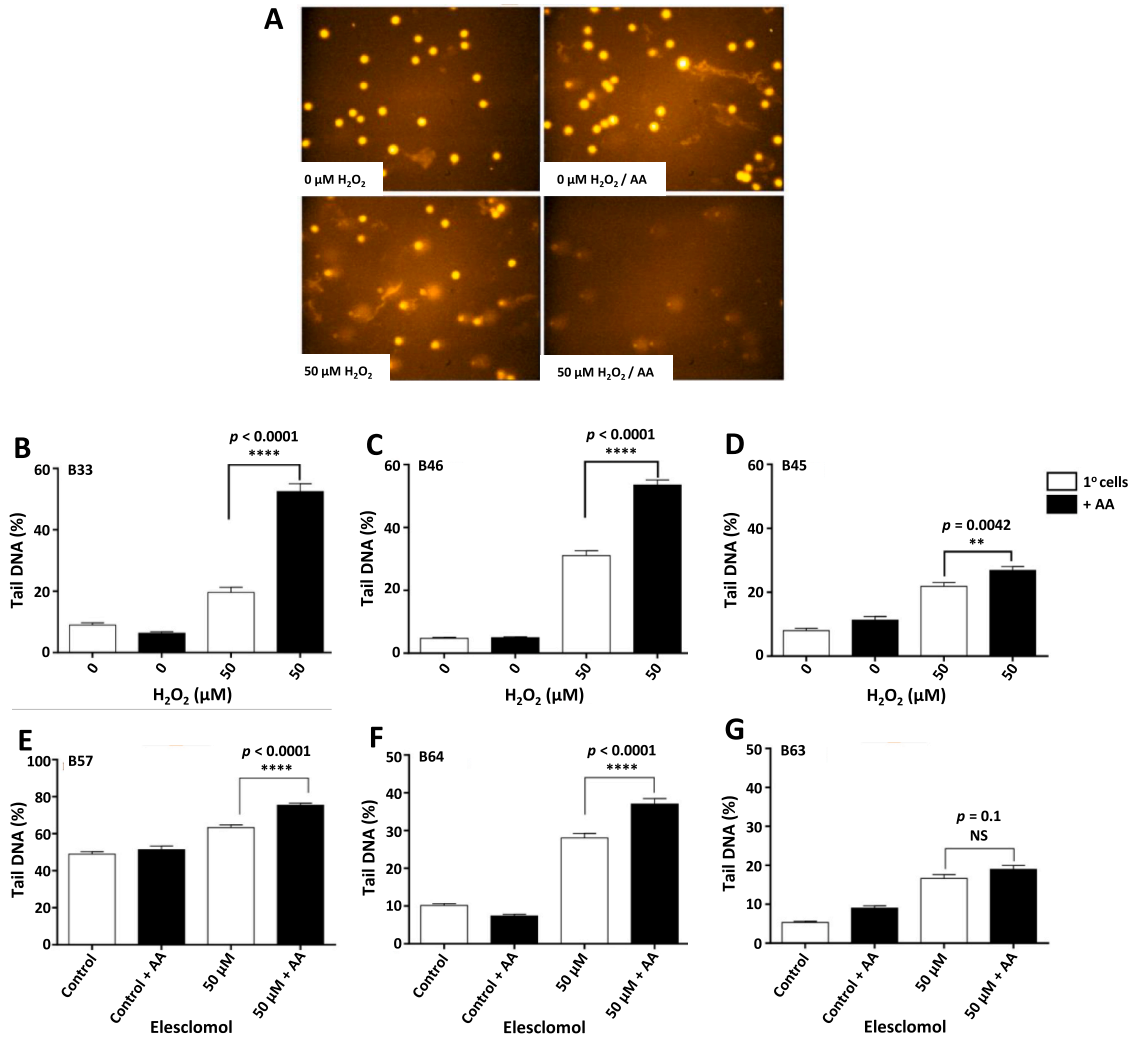

Fig. 5. Ascorbate enhances H_2O_2 and Elesclomol-induced DNA damage formation in primary MM cell cultures *ex vivo*. A). Fluorescent images of comets induced by H_2O_2, following pre-treatment with or without ascorbate, in primary (1^o) MM cultures derived from B33. **B-G).** Prepared 1^o MM tissue cultures (pigmented: B33 **B**, B46 **C**, B57 **E** & B64 **F** and non-pigmented: B45 **D** & B63 **G**) were treated with and without ascorbate (100 μM) then exposed to either 50 μM H_2O_2 for 30 min on ice (B–D), or to Elesclomol for 15 h at 37 °C/5 % CO_2 (E–G) and standard ACA was performed. Each bar represents the mean Tail DNA (%) of 300 comets + SEM. The T-test (unpaired) was used for statistical analysis between each group (ascorbate treated versus ascorbate untreated cells); NS, non-significant, $^{**}p < 0.01$, $^{****}p < 0.0001$.

cytoskeletal-targeting drug with a mechanism of action that is entirely independent of Elesclomol-induced oxidative stress [94–96]. Therefore, presently we examined Elesclomol-induced DNA damage formation in MM cells in the presence and absence of ascorbate, which we have already shown is able to enhance oxidant-induced DNA damage formation in MM cells.

Our results indicate that ascorbate significantly promotes Elesclomol-induced DNA damage in MM cells, particularly in heavily pigmented SK23 cells (Fig. 4D). Furthermore, Fpg-ACA analysis revealed ascorbate-enhanced ODPNL formation in heavily pigmented SK23 cells, confirming the enhancement of Elesclomol-induced oxidatively damaged DNA in MM cells by ascorbate.

Extending the above studies, primary melanoma cell cultures were investigated *ex vivo* to assess ascorbate modulation of H_2O_2 and Elesclomol-induced DNA damage. Use of primary cultures should better reflect the cell biology [97,98] of this type of cancer cell and its response to redox-modulation. Cells from six tissue samples (four pigmented and two non-pigmented) were treated with either H_2O_2 or Elesclomol, following pre-treatment with or without ascorbate, and SB levels assessed by ACA. Treatment in the presence ascorbate significantly enhanced the levels of DNA damage induced by both H_2O_2 (Fig. 5B and C) and Elesclomol (Fig. 5E and F) in the pigmented primary cultures compared to the non-pigmented primary cultures (Fig. 5D and G).

Taken together, our results suggest an improved therapeutic potential for Elesclomol when in combination with ascorbate. Thus, the findings of previous clinical trials should not discourage the possibility of Elesclomol offering utility as a therapy for mediating oxidative stress in melanoma tissue.

In conclusion, the data presented here using primary melanoma cancer cells is consistent with our data using cultured melanoma cancer cells. Ultimately, ascorbate has the capacity to modulate oxidative-stress mediated DNA damage induced by the exogenously applied oxidant H_2O_2 and Elesclomol in melanoma cancer. Moreover, the extent of oxidatively damaged DNA in melanoma cells matches the extent of melanin pigmentation. As such, the benefits of this study primarily relate to the possibility of using ascorbate in ROS-mediated combination therapy to treat melanoma cancer.

4. Materials and methods

4.1. Chemicals and reagents

All chemicals and reagents (including cell media) were purchased from either Sigma-Aldrich/Merck or Life Technologies unless otherwise stated.

The required concentrations of ascorbate for treatment were prepared from a freshly prepared 10 mM stock of L-ascorbate, prepared in calcium-, magnesium-, sodium pyruvate- and Phenol Red-free sterile-filtered PBS (pH 7.4) and held at 4 °C prior to use. The AA stock was prepared fresh on the day of each experiment using 18 mΩ water and dedicated acid-washed stoppered light-tight volumetric glassware.[4]

4.2. Cell lines and culture

Four established human melanoma cancer cell lines, including two non-pigmented (A375M and A375P), a moderately pigmented (SK-MEL-28 (SK28)) and a heavily pigmented (SK-MEL-23 (SK23)) cell line, plus immortalized human keratinocytes (HaCaTs) were obtained from the Leicester Cancer Research cell-bank. All cell lines were determined to be free from mycoplasma contamination and were routinely maintained as monolayer cultures, incubated at 37 °C under 5 % CO_2. A375M, A375P and SK23 MM cells were cultured using Roswell Park Memorial Institute-1640 (RPMI-1640) culture medium, supplemented with 10 % fetal calf serum (FCS) and 1 % glutamax. SK28 cells were cultured using Dulbecco's Modified Eagle's Medium (DMEM), supplemented with 1 % non-essential amino acids (NEAA), 10 % FCS, 1 % glutamax and 1 % sodium pyruvate. HaCaT cells were cultured in DMEM supplemented with 10 % FCS, 1 % sodium pyruvate and 1 % glutamax. For routine sub-culturing cells were trypsinised for 3–5 min using 1 x trypsin-EDTA (0.05 % trypsin, 0.7 mM EDTA) at 37 °C. Once the cells were detached, cell-specific media containing 10 % foetal bovine serum (FBS) was added to halt trypsinisation. Cells were then centrifuged (2000×*g*), counted/viability assessed (Trypan blue) and the required cell number seeded into flasks in cell-specific media for continued culturing or into 6-well plates for treatment.

4.3. Primary tissue cultures

MM tissue samples were obtained via the Cancer Research Biobank, University of Leicester, following favourable NHS research ethics committee review (approval number 13/EM/0196). Melanoma tumour samples were taken via routine surgical excision of both skin and lymph node MM metastases from MM patients at the Leicester Royal Infirmary and were used to make primary tissue cultures. Surrounding stroma and necrotic tissue was dissected from the tumour by a histopathologist to produce samples of enriched melanoma tumour cells. Samples were then immediately placed in media 199 (Thermo Fisher Scientific) on ice to support tumour cell viability for transport to the lab. Upon lab arrival, cell disaggregation was initiated by the mincing of samples into small pieces ($\leq$ 1 mm^2) and collected into 15 mL tubes. 5 mL of media 199 containing Liberase TM (LIBTM) Research Grade (60 μg/mL) (Roche) was added and the samples mixed constantly on an agitating platform at 37 °C. The cell suspension was then centrifuged and the supernatant removed. 5 mL of Hank's Balanced Salt Solution (HBSS) with 2 % FBS was then added to the pellet and mixed thoroughly to neutralise the effect of the LIBTM. The cells were then counted/viability assessed (Trypan blue) to achieve the required number of tumour cells in Eppendorf tubes for treatment.

4.4. Treatment of cells with test compounds

For the treatment of adherent cells with ascorbate, the cell-bearing 6-well plates (seeded the afternoon before with 20 × 10^4 cells per well and left to incubate overnight before treatment) were washed once with sterile pre-warmed PBS (pH 7.4) and then fresh cell-specific media (3 mL) containing the required concentrations of ascorbate was added and incubated at 37 °C/5 % CO_2 for 2 h; control samples were incubated in media alone. Following treatment, cells were washed once with PBS (pH 7.4) ready for H_2O_2 or Elesclomol treatment; Elesclomol (STA-4783) was purchased from Selleckchem.

For the ascorbate treatment of isolated primary MM cell cultures in Eppendorf tubes, 4 × 10^4 cells were treated with media 199 (1.5 mL) containing 100 μM ascorbate and incubated at 37 °C/5 % CO_2 for 2 h. After treatment, cells were washed once with PBS and centrifuged to obtain a pellet ready for H_2O_2 or Elesclomol treatment.

From the supplied H_2O_2 stock solution (30 % w/w; 9.79 M) a 1 mM stock of H_2O_2 was prepared using fresh PBS (pH 7.4). Prior to each experiment, the desired H_2O_2 treatment concentrations were prepared using pre-warmed serum-free RPMI-1640 media and protected from light. Throughout this study serum-free RPMI-1649 media was used for the exposure of cells to H_2O_2. Preliminary studies demonstrated an inhibitory effect on H_2O_2-induced DNA damage when using media containing pyruvic acid (i.e. DMEM); this is supported by the finding of Long et al. [99] which reports that media containing pyruvate serves to scavenge hydrogen peroxide. So, for the treatment of established cells with H_2O_2, cell-specific media was removed and the cells washed twice with pre-warmed PBS (pH 7.4) and then treated with serum-free RPMI-1640 media containing required concentrations of H_2O_2, on ice for 30 min, protected from light. Following treatment, the media was removed and the cells washed once with PBS (pH 7.4) and the desired number placed in pre-labelled Eppendorf tubes on ice in preparation for Comet assay analysis. For γ-H2AX immunoassay (see below), the seeded cells on coverslips were treated as described above.

The pellets of the ascorbate treated primary MM cell cultures in Eppendorf tubes were suspended in serum-free RPMI-1640 media containing H_2O_2 and samples were kept on ice for 30 min protected from light. The media containing H_2O_2 was then removed by centrifugation (2000×*g*).

The Elesclomol stock solutions (10 mM) were prepared using dimethyl sulfoxide (DMSO) and then further diluted using serum-free RPMI-1640 media to obtain the desired drug concentration. For the treatment of adherent cells with Elesclomol, media from each well of a 6-well plate was removed and the cells washed with pre-warmed sterile PBS (pH 7.4). Serum-free RPMI-1640 media containing Elesclomol was then added to the cells and incubated at 37 °C/5 % CO_2 for the specified periods of time. As control and negative controls, cells were incubated with medium containing DMSO alone or 500 μM of N-Acetyl-L-Cysteine (NAC) (for 30 min at 37 °C/5 % CO_2) following Elesclomol treatment, respectively (Fig. 4A). For the treatment of primary MM cell cultures with Elesclomol, suspended cells were washed once with PBS after treatment with ascorbate. Cells were then incubated with serum-free RPMI-1640 media containing Elesclomol for the specified times at 37 °C/5 % CO_2.

4.5. Standard and Fpg-modified alkaline comet assay

DNA damage in the form of SBs + ALS and oxidatively damaged purine nucleobase lesions (ODPNLs) were measured via standard and Fpg-ACA, respectively (ODPNLs being assessed as Fpg-ss). The standard ACA was run according to general protocol of Singh et al. [100] as detailed by Zainol et al. [101]. For the modified ACA, formamidopyrimidine glycosylase (Fpg) (New England Biolabs) enzyme was used to digest the lysis-generated nucleoid body DNA as follows:

[4] For further details of how to best prepare and handle aqueous solutions of ascorbate for basic research and *in vivo* administration see: Wagner & Buettner [2023] 'Stability of aqueous solutions of ascorbate for basic research and for intravenous administration' *Advances in Redox Research* Volume 9, December 2023, 100077.

following overnight lysis, each slide-mounted gel was washed three times with 50 μL of the supplied 1x Enzyme reaction buffer (ERB) for 5 min. Each gel was then treated with 50 μL of appropriately diluted Fpg in 1x ERB, with a cover slip applied to spread the diluted Fpg evenly over the gel, and the slides incubated at 37 °C in humidified light-tight boxes for 30 min. The slides were then placed in the electrophoresis tank and electrophoresis run and comets scored as described [101]. For the visualisation and scoring of comets, Comet Assay software (Version 4.2, Instem) was used to capture and analyse comet images. 50 comets were randomly selected from six gels (from three slides of two gels per slide) yielding 300 comets, and 'percentage tail DNA' (Tail DNA (%)) recorded as the most accurate/robust measure of DNA damage [102].

4.6. γ-H2AX immunoassay

The level of DSBs in treated cells was determined by a γ-H2AX immunoassay. Cells were seeded and grown on sterile cover slips in 6-well plates (2×10^4 cells per well) and left overnight at 37 °C/5 % CO_2. Cells were then pre-incubated for 2 h with ascorbate, then washed with ice-cold PBS before exposure to various micromolar concentrations of H_2O_2 (prepared in serum free RPMI-1640 medium) on ice for 30 min, protected from light. Cells were then washed with PBS and fixed in 100 % methanol for 24 h at −20 °C. Following methanol removal, cells were washed twice for 10 min each in ice-cold PBS and then incubated for 15 min in KCM blocking buffer (0.12 M KCl, 20 mM NaCl, 10 mM Tris-HCl and 1 mM EDTA with 2 % of BSA (w/v), 10 % (w/v) normal goat serum, 10 % (w/v) goat milk powder with 0.1 % (v/v) Triton X-100 added fresh).

Following the removal of the KCM blocking buffer, the primary anti-phosphohistone H2AX (ser^{139}) antibody (Clone JBW301, Mouse Monoclonal Antibody; Thermo Fisher Scientific) was diluted in blocking buffer to 5 μg/mL and added to the cells and incubated for 2 h on a shaker at room temperature. Cells were then washed four times with KCM washing buffer (0.12 M KCl, 20 mM NaCl, 10 mM Tris-HCl and 1 mM EDTA with 0.1 % (v/v) Triton X-100 added fresh). The secondary antibody (A21121 Alexa Fluor 488 Goat Antimouse IgG; Thermo Fisher Scientific), diluted in blocking buffer to the same concentration as the primary antibody, was added to the cells, and incubated for 1 h on a shaker at room temperature. Finally, cells were washed four times using KCM washing buffer and then a drop of SlowFade® Gold antifade reagent (Thermo Fisher Scientific) with DAPI (10 μL) was dispensed on each labelled slide, and the cover slip then mounted upside down on labelled glass microscope slides (the treated cells being between the cover slip and the slide surface). After the slides had been dried at room temperature, they were stored at 4 °C for 24 h ready for image analysis.

To count foci (centres of DSB-induced hyperphosphorylated γ-H2AX) number per cell, a fluorescent Zeiss Axioskop 2 plus microscope, with an Axio-CamHRc camera (Zeiss) with Axio-Vision software, at 40X magnification was used to produce images of treated cells. The analysis of the captured images was carried out using ImageJ (WCIF Image J version 1.42, available from Research Services branch of NIH). From each sample, 10 fields of view (*ca.* 400 cells in total) were randomly chosen for analysis. Images of clear γ-H2AX foci were captured using a 485 μM filter, whereas the number of DAPI stained nuclei images were captured using a DAPI filter. As a part of the ImageJ software's functioning, γ-H2AX foci and nuclei numbers were counted automatically. After exclusion of cells with more than one nucleus, the actual numbers of γ-H2AX foci per cell (DAPI nuclei) were obtained by dividing the total number of γ-H2AX foci by the total number of cells per field.

4.7. Measurement of intracellular oxidising species by plate reader

Cells were seeded in 96-microwell black plates (ca. 8.5×10^4 cells/per well) and incubated at 37 °C/5 % CO_2 for 24 h. Cells were then washed with 200 μL PBS (pH 7.4) and 1 μL of 25 mM fluorescent dye 2′,7′-Dichlorodihydrofluorescein diacetate (H_2DCFDA) in DMSO was added to each well (blank, controls and samples) and the plate covered and incubated for 30 min at 37 °C. 200 μL of PBS was then added to each well and a fluorometric plate reader 76 (BMG FLUOstar OPTIMA Microplate Reader) was immediately used to determine relative DCF fluorescence intensity at an excitation of 480 nm and emission of 530 nm.

4.8. Measurement of intracellular oxidising species by flow cytometry

Cells were seeded in 6-well plates (ca. 5×10^5 cells/well) and incubated at 37 °C/5 % CO_2 for 24 h H_2DCFDA dye was diluted with DMSO (10 mg/mL), with a minimal exposure to air, then 0.5 μL of diluted H_2DCFDA per 1 mL of media was added to cells and incubated for 30 min at 37 °C. Cells were then washed with PBS (pH 7.4), harvested (trypsinisation 0.5 mL/well), centrifuged, re-suspended in 0.5 mL PBS (pH 7.4), transferred to FACS tubes and kept at 4 °C protected from light until analysis by flow cytometry. DCF fluorescence at 530 nm was measured by flow cytometry as described by Eruslanov et al. [103].

4.9. Measurement of total intracellular iron levels

Total intracellular iron ion levels were measured in MM cells using a colorimetric iron assay kit according to the manufacturer's instructions (Abacam). Briefly, MM cells (A375P and SK23) were cultured in a T175 flask at 37 °C/5 % CO_2 until ca. 80 % confluent. After washing with PBS (pH 7.4) and trypsinisation (without EDTA), cells were collected in 15 mL centrifuge tubes then washed twice with PBS (pH 7.4) and centrifuged again. To lyse the cells, pellets of 2×10^6 cells was mixed with 250 μL of the supplied assay buffer. The mixture was centrifuged at 16,000×*g* for 10 min to remove insoluble material and the supernatant was pipetted into a sterile Eppendorf tube. Different volumes (0, 2, 4, 6, 8, and 10 μL) of a diluted iron standard solution (1 mM, freshly prepared from the supplied iron standard stock) was added to empty microwells of a 96 well plate; similarly, different volumes of cell lysate were added to the microwells with the volume of the iron standards and samples in each microwell being made-up to 100 μL with assay buffer. Next, 5 μL of supplied iron reducer was added to each well and the plate was incubated for 30 min at room temperature. 100 μL of supplied iron probe (Ferene S) was then added to each microwell and again the plate was incubated at room temperature for 60 min, protected from light. The optical density at 593 nm, of the plate was then measured.

4.10. Clonogenic cell survival assay

Clonogenic assay was used to assess cell reproductive integrity; a cell's ability to grow and form colonies consisting of at least 50 individual cells after being treated. 5×10^4 cells/well were seeded into 6-well plates and incubated for 24 h at 37 °C/5 % CO_2. After being exposed to the treatment(s) under investigation, the cells were washed with PBS (pH 7.4), harvested, counted and seeded in 9 cm labelled petri dishes. The number of seeded cells varied depending on the plate efficiency (PE) of each cell line, and ranged from 50 to 200 cells. Fresh cell-specific complete media was added to each Petri dish and incubated at 37 °C/5 % CO_2 until small colonies were observed; old media being replaced with fresh complete media every six days. When visible colonies appeared, media was removed and the colonies 'fixed' with 2 mL of 100 % ethanol for 1 min. The plates were then gently rinsed with water and left overnight to dry at room temperature. The following day, each plates' colonies was stained by adding 2 mL of 0.5 % crystal violet for 1 min. Plates were then re-washed with water and left for 3 h to dry at room temperature. Colonies were then counted and recorded for each plate thus enabling calculations for plating efficiency and cell survival (%).

4.11. Catalase activity assay

Assessment of catalase activity was carried out using a simple qualitative method, as described by Iwase et al. [59]. Cells were seeded in T175 flasks and incubated for 3–4 days to yield a suitable number of cells for this assay (1×10^6–1×10^7 cells per sample). The cells were washed twice with sterile pre-warmed PBS (pH 7.4), harvested & counted (trypan blue) and the required cell numbers aliquoted into 15 mL tubes, centrifuged (4 min; 4000×*g*) then washed twice with sterile pre-warmed PBS (pH 7.4) and again centrifuged. Cells from each tube were suspended with 100 μL PBS, mixed thoroughly and placed into labelled Pyrex tubes. To each suspension, 100 μL of 1 % Triton-X 100 and 100 μL of concentrated H_2O_2 (30 %) were added, thoroughly mixed and left for 3 min at room temperature. Cellular catalase reacts with H_2O_2 forming an O_2-foam in the Pyrex tubes, and the height of O_2-foam, representing catalase activity, was then measured.

4.12. Statistical analysis

Statistical differences among sample groups were determined using GraphPad Prism software version 6 (San Diego, CA, USA). Statistical differences between means for multiple comparisons was determined via One-Way Analysis of Variance (ANOVA) followed by Tukey post hoc test. To compare the difference between two comparisons a student T-test (unpaired) was used. The probability value (p) was considered as significant if ≤ 0.05 as follows: * if $p \leq 0.05$; ** if $p \leq 0.01$; *** if $p \leq 0.001$; **** if $p \leq 0.0001$: NS, non-significant.

Declaration of interests

The authors declare that they have no known competing financial interests or personal relationships that could have appeared to influence the work reported in this paper.

CRediT authorship contribution statement

Hishyar A. Najeeb: Writing – review & editing, Writing – original draft, Visualization, Investigation, Formal analysis. **Timi Sanusi:** Writing – review & editing, Writing – original draft, Visualization. **Gerald Saldanha:** Writing – review & editing, Writing – original draft, Resources. **Karen Brown:** Writing – review & editing, Writing – original draft, Supervision, Funding acquisition, Conceptualization. **Marcus S. Cooke:** Writing – review & editing, Writing – original draft, Validation, Conceptualization. **George DD. Jones:** Writing – original draft, Visualization, Validation, Supervision, Resources, Project administration, Funding acquisition, Conceptualization.

Acknowledgments

This work was supported by the National Institute for Health and Care Research and Cancer Research UK through Experimental Cancer Medicine Centre (ECMC) awards [C10604/A25151]. We acknowledge Kurdistan Regional Government, Iraq for funding the PhD studentship awarded to HAN and the University of Leicester's Medical School LINK initiative in supporting TS's involvement in this study. We also acknowledge Prof Donald JL Jones, Dr Yii NgiWieh, Karen Kalbicki, Prof Salvador Macip, Dr Jesvin Samuel, Dr Karen Bowman and Dr Alessandro Rufini for their advice and assistance throughout this project.

References

[1] K.V. Laikova, V.V. Oberemok, A.M. Krasnodubets, N.V. Gal'chinsky, R. Z. Useinov, I.A. Novikov, et al., Advances in the Understanding of skin cancer: Ultraviolet Radiation, mutations, and antisense oligonucleotides as anticancer drugs, Molecules (Basel, Switzerland) 24 (8) (2019) 1516.

[2] A. Memon, P. Bannister, I. Rogers, J. Sundin, B. Al-Ayadhy, P.W. James, et al., Changing epidemiology and age-specific incidence of cutaneous malignant melanoma in England: an analysis of the national cancer registration data by age, gender and anatomical site, 1981–2018, The Lancet Regional Health - Europe 2 (2021) 100024.

[3] C.R. UK, Melanoma skin cancer incidence statistics: cancer Research UK; 2015-2017 [Available from: https://www.cancerresearchuk.org/health-professional/cancer-statistics/statistics-by-cancer-type/melanoma-skin-cancer/incidence.

[4] C.R. UK, Melanoma skin cancer survival: cancer research UK; 2020 [Available from: https://www.cancerresearchuk.org/about-cancer/melanoma/survival.

[5] M. Polkowska, P. Ekk-Cierniakowski, E. Czepielewska, M. Kozłowska-Wojciechowska, Efficacy and safety of BRAF inhibitors and anti-CTLA4 antibody in melanoma patients—real-world data, Eur. J. Clin. Pharmacol. 75 (3) (2019) 329–334.

[6] P.B. Chapman, A. Hauschild, C. Robert, J.B. Haanen, P. Ascierto, J. Larkin, et al., Improved survival with vemurafenib in melanoma with BRAF V600E mutation, N. Engl. J. Med. 364 (26) (2011) 2507–2516.

[7] J.A. Sosman, K.B. Kim, L. Schuchter, R. Gonzalez, A.C. Pavlick, J.S. Weber, et al., Survival in BRAF V600–mutant advanced melanoma treated with vemurafenib, N. Engl. J. Med. 366 (8) (2012) 707–714.

[8] C. Luo, J. Shen, Research progress in advanced melanoma, Cancer Lett. 397 (2017) 120–126.

[9] L.E. Davis, S.C. Shalin, A.J. Tackett, Current state of melanoma diagnosis and treatment, Cancer Biol. Ther. 20 (11) (2019) 1366–1379.

[10] J. Verrax, R.C. Pedrosa, R. Beck, N. Dejeans, H. Taper, P.B. Calderon, In situ modulation of oxidative stress: a novel and efficient strategy to kill cancer cells, Curr. Med. Chem. 16 (15) (2009) 1821–1830.

[11] H. Pelicano, D. Carney, P. Huang, ROS stress in cancer cells and therapeutic implications, Drug Resist. Updates 7 (2) (2004) 97–110.

[12] R.A. Cairns, I.S. Harris, T.W. Mak, Regulation of cancer cell metabolism, Nat. Rev. Cancer 11 (2) (2011) 85–95.

[13] C. Nicco, A. Laurent, C. Chereau, B. Weill, F. Batteux, Differential modulation of normal and tumor cell proliferation by reactive oxygen species, Biomed. Pharmacother. 59 (4) (2005) 169–174.

[14] A.A. Konstantinov, A.V. Peskin, E. Popova, G.B. Khomutov, E.K. Ruuge, Superoxide generation by the respiratory chain of tumor mitochondria, Biochim. Biophys. Acta 894 (1) (1987) 1–10.

[15] C.S. Sander, F. Hamm, P. Elsner, J.J. Thiele, Oxidative stress in malignant melanoma and non-melanoma skin cancer, Br. J. Dermatol. 148 (5) (2003) 913–922.

[16] L.J. Marnett, Oxyradicals and DNA damage, Carcinogenesis 21 (3) (2000) 361–370.

[17] M. Valko, C.J. Rhodes, J. Moncol, M. Izakovic, M. Mazur, Free radicals, metals and antioxidants in oxidative stress-induced cancer, Chem. Biol. Interact. 160 (1) (2006) 1–40.

[18] A. Laurent, C. Nicco, C. Chéreau, C. Goulvestre, J. Alexandre, A. Alves, et al., Controlling tumor growth by modulating endogenous production of reactive oxygen species, Cancer Res. 65 (3) (2005) 948–956.

[19] J.A. Sykes, F.X. McCormack, T.J. Brien, A preliminary study of the superoxide dismutase content of some human tumors, Cancer Res. 38 (9) (1978) 2759.

[20] M. Valko, D. Leibfritz, J. Moncol, M.T. Cronin, M. Mazur, J. Telser, Free radicals and antioxidants in normal physiological functions and human disease, Int. J. Biochem. Cell Biol. 39 (1) (2007) 44–84.

[21] I.I.C. Chio, D.A. Tuveson, ROS in cancer: the burning question, Trends Mol. Med. 23 (5) (2017) 411–429.

[22] M. Zalewska-Ziob, B. Adamek, J. Kasperczyk, E. Romuk, E. Hudziec, E. Chwalińska, et al., Activity of antioxidant enzymes in the tumor and adjacent noncancerous tissues of non-small-cell lung cancer, Oxid. Med. Cell. Longev. 2019 (2019) 2901840.

[23] F.M. Nathan, V.A. Singh, A. Dhanoa, U.D. Palanisamy, Oxidative stress and antioxidant status in primary bone and soft tissue sarcoma, BMC Cancer 11 (2011) 382.

[24] H. Sies, Oxidative stress: a concept in redox biology and medicine, Redox Biol. 4 (2015) 180–183.

[25] H. Sies, Hydrogen peroxide as a central redox signaling molecule in physiological oxidative stress: oxidative eustress, Redox Biol. 11 (2017) 613–619.

[26] P.A. Cerutti, Prooxidant states and tumor promotion, Science 227 (4685) (1985) 375–381.

[27] D. Trachootham, J. Alexandre, P. Huang, Targeting cancer cells by ROS-mediated mechanisms: a radical therapeutic approach? Nat. Rev. Drug Discov. 8 (7) (2009) 579–591.

[28] P.T. Schumacker, Reactive oxygen species in cancer cells: live by the sword, die by the sword, Cancer Cell 10 (3) (2006) 175–176.

[29] P. Huang, L. Feng, E.A. Oldham, M.J. Keating, W. Plunkett, Superoxide dismutase as a target for the selective killing of cancer cells, Nature 407 (6802) (2000) 390–395.

[30] F.L. Meyskens Jr., H.V. Chau, N. Tohidian, J. Buckmeier, Luminol-enhanced chemiluminescent response of human melanocytes and melanoma cells to hydrogen peroxide stress, Pigm. Cell Res. 10 (3) (1997) 184–189.

[31] F.A. Offner, H.C. Wirtz, J. Schiefer, I. Bigalke, B. Klosterhalfen, F. Bittinger, et al., Interaction of human malignant melanoma (ST-ML-12) tumor spheroids with endothelial cell monolayers. Damage to endothelium by oxygen-derived free radicals, Am. J. Pathol. 141 (3) (1992) 601–610.

[32] M. Picardo, P. Grammatico, F. Roccella, M. Roccella, M. Grandinetti, G. del Porto, et al., Imbalance in the antioxidant pool in melanoma cells and normal melanocytes from patients with melanoma, J. Invest. Dermatol. 107 (3) (1996) 322–326.

[33] F.L. Meyskens Jr., P. Farmer, J.P. Fruehauf, Redox regulation in human melanocytes and melanoma, Pigm. Cell Res. 14 (3) (2001) 148–154.
[34] J.P. Fruehauf, S. Zonis, M. al-Bassam, A. Kyshtoobayeva, C. Dasgupta, T. Milovanovic, et al., Melanin content and downregulation of glutathione S-transferase contribute to the action of L-buthionine-S-sulfoximine on human melanoma, Chem. Biol. Interact. 111–112 (1998) 277–305.
[35] F.L. Meyskens Jr., P.J. Farmer, H. Anton-Culver, Etiologic pathogenesis of melanoma: a unifying hypothesis for the missing attributable risk, Clin. Cancer Res. 10 (8) (2004) 2581–2583.
[36] H.T. Wang, B. Choi, M.S. Tang, Melanocytes are deficient in repair of oxidative DNA damage and UV-induced photoproducts, Proc. Natl. Acad. Sci. U. S. A. 107 (27) (2010) 12180–12185.
[37] S. Gidanian, P.J. Farmer, Redox behavior of melanins: direct electrochemistry of dihydroxyindole-melanin and its Cu and Zn adducts, J. Inorg. Biochem. 89 (1–2) (2002) 54–60.
[38] B. Szpoganicz, S. Gidanian, P. Kong, P. Farmer, Metal binding by melanins: studies of colloidal dihydroxyindole-melanin, and its complexation by Cu(II) and Zn(II) ions, J. Inorg. Biochem. 89 (1–2) (2002) 45–53.
[39] C. Sarzanini, E. Mentasti, O. Abollino, M. Fasano, S. Aime, Metal ion content in Sepia officinalis melanin, Mar. Chem. 39 (4) (1992) 243–250.
[40] S.S. Shapiro, C. Saliou, Role of vitamins in skin care, Nutrition 17 (10) (2001) 839–844.
[41] J.M. May, Ascorbate function and metabolism in the human erythrocyte, Front. Biosci. 3 (1998) d1–d10.
[42] J. Verrax, P.B. Calderon, The controversial place of vitamin C in cancer treatment, Biochem. Pharmacol. 76 (12) (2008) 1644–1652.
[43] B. Halliwell, A. Adhikary, M. Dingfelder, M. Dizdaroglu, Hydroxyl radical is a significant player in oxidative DNA damage in vivo, Chem. Soc. Rev. 50 (2021) 8355–8360.
[44] M.G. Simic, S.V. Jovanovic, Free radical mechanisms of DNA base damage, in: M. G. Simic, L. Grossman, A.C. Upton, D.S. Bergtold (Eds.), Mechanisms of DNA Damage and Repair: Implications for Carcinogenesis and Risk Assessment, Springer US, Boston, MA, 1986, pp. 39–49.
[45] S. Loft, H.E. Poulsen, Cancer risk and oxidative DNA damage in man, J. Mol. Med. (Berl.) 74 (6) (1996) 297–312.
[46] H.F. Stick, J. Karim, J. Koropatnick, L. Lo, Mutagaenic action of ascorbic acid, Nature 260 (5553) (1976) 722–724.
[47] T.L. Duarte, G.D. Jones, Vitamin C modulation of H2O2-induced damage and iron homeostasis in human cells, Free Radic. Biol. Med. 43 (8) (2007) 1165–1175.
[48] K. Satoh, H. Sakagami, Effect of metal ions on radical intensity and cytotoxic activity of ascorbate, Anticancer Res. 17 (2a) (1997) 1125–1129.
[49] S.L. Baader, G. Bruchelt, T.C. Carmine, H.N. Lode, A.G. Rieth, D. Niethammer, Ascorbic-acid-mediated iron release from cellular ferritin and its relation to the formation of DNA strand breaks in neuroblastoma cells, J. Cancer Res. Clin. Oncol. 120 (7) (1994) 415–421.
[50] C. Badu-Boateng, R.J. Naftalin, Ascorbate and ferritin interactions: consequences for iron release in vitro and in vivo and implications for inflammation, Free Radic. Biol. Med. 133 (2019) 75–87.
[51] K. Sakurai, A. Nabeyama, Y. Fujimoto, Ascorbate-mediated iron release from ferritin in the presence of alloxan, Biometals 19 (3) (2006) 323–333.
[52] M. Ozaki, T. Kawabata, M. Awai, Iron release from haemosiderin and production of iron-catalysed hydroxyl radicals in vitro, Biochem. J. 250 (2) (1988) 589–595.
[53] J. Hunyady, The result of vitamin C treatment of patients with cancer: conditions influencing the effectiveness, Int. J. Mol. Sci. 23 (8) (2022).
[54] T.L. Duarte, G.M. Almeida, G.D.D. Jones, Investigation of the role of extracellular H2O2 and transition metal ions in the genotoxic action of ascorbic acid in cell culture models, Toxicol. Lett. 170 (1) (2007) 57–65.
[55] Q. Chen, M.G. Espey, M.C. Krishna, J.B. Mitchell, C.P. Corpe, G.R. Buettner, et al., Pharmacologic ascorbic acid concentrations selectively kill cancer cells: action as a pro-drug to deliver hydrogen peroxide to tissues, Proc. Natl. Acad. Sci. U. S. A. 102 (38) (2005) 13604–13609.
[56] S.S. Wallace, Ap endonucleases and dna glycosylases that recognize oxidative dna damage, Environ. Mutagen. 12 (4) (1988) 431–477.
[57] J.H.J. Hoeijmakers, DNA repair mechanisms, Maturitas 38 (1) (2001) 17–22.
[58] J. Navarro, E. Obrador, J. Carretero, I. Petschen, J. Aviñó, P. Perez, et al., Changes in glutathione status and the antioxidant system in blood and in cancer cells associate with tumour growth in vivo, Free Radic. Biol. Med. 26 (3) (1999) 410–418.
[59] T. Iwase, A. Tajima, S. Sugimoto, K. Okuda, I. Hironaka, Y. Kamata, et al., A simple assay for measuring catalase activity: a visual approach, Sci. Rep. 3 (2013) 3081.
[60] A. Barbouti, P.T. Doulias, B.Z. Zhu, B. Frei, D. Galaris, Intracellular iron, but not copper, plays a critical role in hydrogen peroxide-induced DNA damage, Free Radic. Biol. Med. 31 (4) (2001) 490–498.
[61] J.F. Ward, DNA damage produced by ionizing radiation in mammalian cells: identities, mechanisms of formation, and reparability, in: W.E. Cohn, K. Moldave (Eds.), Progress in Nucleic Acid Research and Molecular Biology, vol. 35, Academic Press, 1988, pp. 95–125.
[62] J.R. Kirshner, S. He, V. Balasubramanyam, J. Kepros, C.Y. Yang, M. Zhang, et al., Elesclomol induces cancer cell apoptosis through oxidative stress, Mol. Cancer Therapeut. 7 (8) (2008) 2319–2327.
[63] A. Berkenblit, J.P. Eder Jr., D.P. Ryan, M.V. Seiden, N. Tatsuta, M.L. Sherman, et al., Phase I clinical trial of STA-4783 in combination with paclitaxel in patients with refractory solid tumors, Clin. Cancer Res. 13 (2 Pt 1) (2007) 584–590.
[64] J. Powderly, K. Khan, J. Richards, W. Urba, M. McLeod, T. Dahl, et al., A 2-stage controlled phase 1/2 study of STA-4783 in combination with paclitaxel in patients with advanced metastatic melanoma, J. Clin. Oncol. 23 (16_suppl) (2005) 7561.
[65] S. O'Day, R. Gonzalez, D. Lawson, R. Weber, L. Hutchins, C. Anderson, et al., Phase II, randomized, Controlled, Double-blinded Trial of weekly Elesclomol Plus paclitaxel versus paclitaxel alone for stage IV metastatic melanoma, J. Clin. Oncol. 27 (32) (2009) 5452–5458.
[66] S.J. O'Day, A.M.M. Eggermont, V. Chiarion-Sileni, R. Kefford, J.J. Grob, L. Mortier, et al., Final results of phase III SYMMETRY study: randomized, double-blind trial of elesclomol plus paclitaxel versus paclitaxel alone as treatment for chemotherapy-naive patients with advanced melanoma, J. Clin. Oncol. 31 (9) (2013) 1211–1218.
[67] M. Nagai, N.H. Vo, L. Shin Ogawa, D. Chimmanamada, T. Inoue, J. Chu, et al., The oncology drug elesclomol selectively transports copper to the mitochondria to induce oxidative stress in cancer cells, Free Radic. Biol. Med. 52 (10) (2012) 2142–2150.
[68] R.K. Blackman, K. Cheung-Ong, M. Gebbia, D.A. Proia, S. He, J. Kepros, et al., Mitochondrial electron transport is the cellular target of the oncology drug elesclomol, PLoS One 7 (1) (2012) e29798.
[69] M. Cierlitza, H. Chauvistre, I. Bogeski, X. Zhang, A. Hauschild, M. Herlyn, et al., Mitochondrial oxidative stress as a novel therapeutic target to overcome intrinsic drug resistance in melanoma cell subpopulations, Exp. Dermatol. 24 (2) (2015) 155–157.
[70] H. Shi, W. Hugo, X. Kong, A. Hong, R.C. Koya, G. Moriceau, et al., Acquired resistance and clonal evolution in melanoma during BRAF inhibitor therapy, Cancer Discov. 4 (1) (2014) 80.
[71] A.M. Menzies, L.E. Haydu, M.S. Carlino, M.W. Azer, P.J. Carr, R.F. Kefford, et al., Inter- and intra-patient heterogeneity of response and progression to targeted therapy in metastatic melanoma, PLoS One 9 (1) (2014) e85004.
[72] A. Ghanem, A.M. Melzer, E. Zaal, L. Neises, D. Baltissen, O. Matar, et al., Ascorbate kills breast cancer cells by rewiring metabolism via redox imbalance and energy crisis, Free Radic. Biol. Med. 163 (2021) 196–209.
[73] M. Uetaki, S. Tabata, F. Nakasuka, T. Soga, M. Tomita, Metabolomic alterations in human cancer cells by vitamin C-induced oxidative stress, Sci. Rep. 5 (1) (2015) 13896.
[74] A.R. Gibson, B.R. Leary, J. Du, E.H. Sarsour, A.L. Kalen, B.A. Wagner, et al., Dual oxidase-induced sustained generation of hydrogen peroxide contributes to pharmacologic ascorbate-induced cytotoxicity, Cancer Res. 80 (7) (2020) 1401.
[75] M. Starczak, E. Zarakowska, M. Modrzejewska, T. Dziaman, A. Szpila, K. Linowiecka, et al., In vivo evidence of ascorbate involvement in the generation of epigenetic DNA modifications in leukocytes from patients with colorectal carcinoma, benign adenoma and inflammatory bowel disease, J. Transl. Med. 16 (1) (2018) 204.
[76] R. Yin, S.-Q. Mao, B. Zhao, Z. Chong, Y. Yang, C. Zhao, et al., Ascorbic acid enhances tet-mediated 5-methylcytosine oxidation and promotes DNA demethylation in mammals, J. Am. Chem. Soc. 135 (28) (2013) 10396–10403.
[77] E.A. Minor, B.L. Court, J.I. Young, G. Wang, Ascorbate induces ten-eleven translocation (tet) methylcytosine dioxygenase-mediated generation of 5-hydroxymethylcytosine*◆, J. Biol. Chem. 288 (19) (2013) 13669–13674.
[78] M.S. Alexander, J.G. Wilkes, S.R. Schroeder, G.R. Buettner, B.A. Wagner, J. Du, et al., Pharmacologic ascorbate reduces radiation-induced normal tissue toxicity and enhances tumor radiosensitization in pancreatic cancer, Cancer Res. 78 (24) (2018) 6838–6851.
[79] J. Du, R.S. Carroll, G.J. Steers, B.A. Wagner, B.R. O'Leary, C.S. Jensen, et al., Catalase modulates the radio-sensitization of pancreatic cancer cells by pharmacological ascorbate, Antioxidants 10 (4) (2021).
[80] R. Olinski, T.H. Zastawny, M. Foksinski, A. Barecki, M. Dizdaroglu, DNA base modifications and antioxidant enzyme activities in human benign prostatic hyperplasia, Free Radic. Biol. Med. 18 (4) (1995) 807–813.
[81] C. Glorieux, N. Dejeans, B. Sid, R. Beck, P.B. Calderon, J. Verrax, Catalase overexpression in mammary cancer cells leads to a less aggressive phenotype and an altered response to chemotherapy, Biochem. Pharmacol. 82 (10) (2011) 1384–1390.
[82] A. Guidarelli, M. Fiorani, O. Cantoni, Enhancing effects of intracellular ascorbic acid on peroxynitrite-induced U937 cell death are mediated by mitochondrial events resulting in enhanced sensitivity to peroxynitrite-dependent inhibition of complex III and formation of hydrogen peroxide, Biochem. J. 378 (Pt 3) (2004) 959–966.
[83] A. Guidarelli, R. De Sanctis, B. Cellini, M. Fiorani, M. Dachà, O. Cantoni, Intracellular ascorbic acid enhances the DNA single-strand breakage and toxicity induced by peroxynitrite in U937 cells, Biochem. J. 356 (Pt 2) (2001) 509–513.
[84] E.R. Whittemore, D.T. Loo, C.W. Cotman, Exposure to hydrogen peroxide induces cell death via apoptosis in cultured rat cortical neurons, Neuroreport 5 (12) (1994) 1485–1488.
[85] E. Panieri, V. Gogvadze, E. Norberg, R. Venkatesh, S. Orrenius, B. Zhivotovsky, Reactive oxygen species generated in different compartments induce cell death, survival, or senescence, Free Radic. Biol. Med. 57 (2013) 176–187.
[86] G.F. Jin, J.S. Hurst, B.F. Godley, Hydrogen peroxide stimulates apoptosis in cultured human retinal pigment epithelial cells, Curr. Eye Res. 22 (3) (2001) 165–173.
[87] M. Mendivil-Perez, C. Velez-Pardo, M. Jimenez-Del-Rio, Doxorubicin induces apoptosis in Jurkat cells by mitochondria-dependent and mitochondria-independent mechanisms under normoxic and hypoxic conditions, Anti Cancer Drugs 26 (6) (2015) 583–598.
[88] A. Bressenot, S. Marchal, L. Bezdetnaya, J. Garrier, F. Guillemin, F. Plénat, Assessment of apoptosis by immunohistochemistry to active caspase-3, active

caspase-7, or cleaved PARP in monolayer cells and spheroid and subcutaneous xenografts of human carcinoma, J. Histochem. Cytochem. 57 (4) (2009) 289–300.
[89] E.A. Slee, C. Adrain, S.J. Martin, Executioner caspase-3, -6, and -7 perform distinct, non-redundant roles during the demolition phase of apoptosis, J. Biol. Chem. 276 (10) (2001) 7320–7326.
[90] S.A. Lakhani, A. Masud, K. Kuida, G.A. Porter Jr., C.J. Booth, W.Z. Mehal, et al., Caspases 3 and 7: key mediators of mitochondrial events of apoptosis, Science 311 (5762) (2006) 847–851.
[91] M. Tochigi, T. Inoue, M. Suzuki-Karasaki, T. Ochiai, C. Ra, Y. Suzuki-Karasaki, Hydrogen peroxide induces cell death in human TRAIL-resistant melanoma through intracellular superoxide generation, Int. J. Oncol. 42 (3) (2013) 863–872.
[92] R. Gonzalez, D.H. Lawson, R.W. Weber, L.F. Hutchins, C.M. Anderson, K. N. Williams, et al., Phase II trial of elesclomol (formerly STA-4783) and paclitaxel in stage IV metastatic melanoma (MM): subgroup analysis by prior chemotherapy, J. Clin. Oncol. 26 (15_suppl) (2008) 9036.
[93] A. Hauschild, A.M. Eggermont, E. Jacobson, S.J. O'Day, Phase III, randomized, double-blind study of elesclomol and paclitaxel versus paclitaxel alone in stage IV metastatic melanoma (MM), J. Clin. Oncol. 27 (18_suppl) (2009). LBA9012-LBA.
[94] R. Bharadwaj, H. Yu, The spindle checkpoint, aneuploidy, and cancer, Oncogene 23 (11) (2004) 2016–2027.
[95] D.A. Brito, Z. Yang, C.L. Rieder, Microtubules do not promote mitotic slippage when the spindle assembly checkpoint cannot be satisfied, JCB (J. Cell Biol.) 182 (4) (2008) 623–629.
[96] B.A. Weaver, How Taxol/paclitaxel kills cancer cells, Mol. Biol. Cell 25 (18) (2014) 2677–2681.
[97] D.M. Pastor, L.S. Poritz, T.L. Olson, C.L. Kline, L.R. Harris, W.A. Koltun, et al., Primary cell lines: false representation or model system? a comparison of four human colorectal tumors and their coordinately established cell lines, Int. J. Clin. Exp. Med. 3 (1) (2010) 69–83.
[98] G. Kaur, J.M. Dufour, Cell lines: valuable tools or useless artifacts, Spermatogenesis 2 (1) (2012) 1–5.
[99] L.H. Long, B. Halliwell, Artefacts in cell culture: pyruvate as a scavenger of hydrogen peroxide generated by ascorbate or epigallocatechin gallate in cell culture media, Biochem. Biophys. Res. Commun. 388 (4) (2009) 700–704.
[100] N.P. Singh, M.T. McCoy, R.R. Tice, E.L. Schneider, A simple technique for quantitation of low levels of DNA damage in individual cells, Exp. Cell Res. 175 (1) (1988) 184–191.
[101] M. Zainol, J. Stoute, G.M. Almeida, A. Rapp, K.J. Bowman, G.D. Jones, Introducing a true internal standard for the Comet assay to minimize intra- and inter-experiment variability in measures of DNA damage and repair, Nucleic Acids Res. 37 (22) (2009) e150.
[102] A. Azqueta, A.R. Collins, The essential comet assay: a comprehensive guide to measuring DNA damage and repair, Arch. Toxicol. 87 (6) (2013) 949–968.
[103] E. Eruslanov, S. Kusmartsev, Identification of ROS using oxidized DCFDA and flow-cytometry, Methods Mol. Biol. 594 (2010) 57–72.